Experimental Study of Natural Convection Heat Transfer in Confined Porous Media Heated From Side

Dr. Abdulhassan A. Karamallah
Professor

Dr. Ihsan Y. Hussain
Professor
drihsan@uobaghdad.edu.iq
dr.ihsanyahya1@yahoo.com

Dr. Dhia-Al-Deen H. Alwan
Lecturer

ABSTRACT

Transient three-dimensional natural convection heat transfer due to the influences of heating from one side of an enclosure filled with a saturated porous media, whereas the opposite side is maintained at a constant cold temperature, and the other four sides are adiabatic, were investigated in the present work experimentally. Silica sand was used as a porous media saturated with distilled water filled in a cubic enclosure heated from the side, using six electrical controlled heaters, at constant temperatures of (60, 70, 80, 90, and 100^{o}C). The inverse side cooled at a constant temperature of (24^{o}C) using an aluminum heat exchanger, consisted of 15 channels feeded with constant temperature water. Eighty thermocouples were used to control the heated and cooled sides, and to measure the temperature in the entire enclosure. Experimental results showed that the heat transfer regime was mainly conduction for all Rayleigh numbers with small influence of convection for *Ra*=42 and greater for Ra=55. This effect increased with the angle of inclination of the enclosure. Numerical and experimental results showed a good agreement. There was a rapid increase in the temperature at the entire media at the early time, reduced gradually until the steady state condition reached. This temperature and heat transfer to and from the porous media, were increased as the Rayleigh number and/or inclination angle increased. The Nusselt number increased directly with the angle of inclination up to $\theta = 45^o$ and then decreased. Correlation equations are obtained from the experimental investigation, showed the change of the average and local Nusselt number with time, distance, Rayleigh number, and the inclination angle.

KEYWORDS : Porous Media, Natural Convection, Side Heating, Experimental Study

الخلاصة

الحمل الحراري الانتقالي الثلاثي الابعاد الناتج عن تأثير التسخين الجانبي لوعاء مكعب مملوء بوسط مسامي مشبع، بينما يكون الجانب الثاني مبرد بدرجة حرارة ثابته والجوانب الاخرى معزولة حراريا هو موضوع البحث العملي الحالي. تم استخدام الرمل كوسط مسامي والماء المقطر للترطيب في صندوق مكعب سخن من الجانب باستخدام ستة ملفات كهربائية مسيطر عليها للحصول على حرارة ثابته (60، 70، 80، 90، 100 درجة مئوية)، بينما تم تثبيت حرارة الجدار المقابل على (24 درجة مئوية) باستخدام مبادل حراري مصنوع من الالمنيوم يحتوي على (15) قناة يزود بالماء ثابت الحرارة. تم استخدام (80) متحسس حراري للسيطرة على درجة الحرارة للسطح البارد والسطح الحار ولمراقبة التغير بالحرارة داخل الوسط المسامي المشبع. النتائج العملية بينت ان انتقال الحرارة يتم بشكل اساسي بالتوصيل في اغلب قيم عدد رايلي مع تأثير قليل للحمل الحر عندما تكون (Ra=42) وبمقدار اكبر عندما تكون (Ra=55). هذا التأثير يزداد مع زيادة ميل زاوية الصندوق. اظهرت الدراسة زيادة مطردة في حرارة الوسط المشبع مع الزمن الابتدائي، تقل هذه الزيادة تدريجيا حتى بلوغ حالة الاستقرار للحرارة في كل الوسط. حرارة الوسط وكمية الحرارة المنتقلة الى داخل الوسط المسامي والخارجة منه تزداد مع زيادة عدد رايلي ومع زيادة زاوية ميل الصندوق المكعب. عدد نسلت يزداد بشكل مباشر مع زاوية الميل حتى بلوغ الميل زاوية (45 درجة) ثم يبدأ بالانخفاض. تم الوصول الى معادلات إرتباط مكتسبة من تحليل النتائج التجريبية، وضحت تغيير كل من عدد نسلت المتوسط ،وعدد نسلت الموضعي مع الوقت، المسافة، عدد رايلي، وزاوية الميل.

INTRODUCTION

The natural convection heat transfer and flow field through fluid-saturated porous media had been a research topic for few decades, although the mechanics of the flow in a porous medium had been the subject of investigations for centuries.

Matters with masses form naturally into porous structures. They occur almost over the entire world at different scales under considerations. Materials with porous structures are called porous media. A porous medium means a material consisting of a solid matrix with interconnected voids. The interconnectedness of the voids (the pores) allows the flow of one or more fluids through the material. In the simplest situation (single-phase flow), the void is saturated by a single fluid. In (two phase flow), a liquid and gas share the void space **(Nield and Bejan 2006)**. How the flows passing through the porous media with the associated heat and mass transfer, has been of a great interest to scientists and engineers for centuries **(Vafai 2005)**.

When the temperature of the saturated fluid phase in a porous medium is not uniform, then flows which are induced by buoyancy effects occur. These flows which depend on the density difference due to the temperature gradients and the pertinent boundary conditions are commonly called free or natural convection. Due to their numerous applications in energy related engineering problem, natural convection has been receiving an increasing amount of interest and it has become one of the most commonly studied transport phenomena in the porous medium.

The analysis of free and forced convection heat transfer in fluid-saturated porous media finds applications in a wide range of environmental and industrial fields including ground water pollution, energy storage in aquifers, biophysical heat transfer, subterranean deposition of heat-generating materials, volcanic and geophysical flows, and etc. To exploit geothermal energy effectively and successfully, engineers require the knowledge of the initiating convection currents in geothermal fluids. In electronic engineering, cooling mechanisms for semi-conductor devices have been modified by the introduction of porous wafer layers. Thermal losses from the receiver of a concentrating solar collector often dominate the performance of the collector system under high temperature operation **(Beg et.al 1998)**.

Fundamental investigations of natural convection heat transfer in saturated porous media appear to have started with a linearized stability theory applied to an infinite horizontal layer heated from below **(Horton and Rogers 1945) m (Lapwood 1948)**. These studies established the criterion for the onset of convection which was experimentally verified by various other investigators later on. Soon thereafter, both analytical and experimental investigations were conducted to determine convective heat transfer rates through saturated permeable media of various geometric shapes, e.g. rectangular, triangular cavities, and horizontal and vertical annuli. Some of these studies were aimed at visualizing the flow field and the temperature distribution as well.

Experimental works have been conducted on porous media by a combination of several fluids and porous beds including various ranges of governing parameters **(Prasad et. Al 1985)**.

Most studies which were done on natural convection in porous media depended on numerical methods to solve the governing equations, limited researches used experimental methods. In these few experimental works, the porous media was almost a spherical particles manufactured from different materials with large diameters, which produced high permeability, saturated with different kinds of liquids, and packed in thin rectangular enclosures. The temperature distribution within the porous media was always taken when the condition of the system reached the steady state. The experimental work of this study assumed the first "unsteady three dimensional" investigation in the field of a single phase natural convection in saturated porous media in a cubic inclined enclosure, packed with silica sand and saturated with distilled water. This experimental work includes the influences range of modified Rayleigh numbers, and inclination angles of the inclosure.

EXPERIMENTAL APPARATUS AND PROCEDURE

The main part of the experimental rig is the cubic inclosure with equal depth, width, and high of 300mm. The left side is heated face while the cooled side is maintained on the inverse face. The remaining four faces are insulated, as depicted in the schematic diagram **Fig. 1**. The heating part shown in **Fig. 2**, maintained on the left side of the test section part, and is consisting of,

1- A pure cupper plate of 5 mm thickness, as the main heat transfer surface to the porous media.

2- The temperature maintained constant at this side by the use of six separated heaters, each heater of (17 ohm) electrical resistance. The heaters are supplied with AC-current from six voltage regulators, to control the current feed to each electrical resistance according to the temperature, measured by six thermocouples maintained in front of each heater. These (0.3 mm) type-T [copper vs. copper-nickel alloy (cupper-constantan)] thermocouples were mounted in the rear side of the copper plates, and the temperature degrees are monitoring by a digital thermometer. A feed back was done to the AC-current regulators according to the temperature read from front of each heater. The heater consists of strips of (1 mm) width made from chrome-nickel alloy with resistance (15 ohm/m) wrapped with (5 mm) pitch around a (50x300 mm^2) mica sheet of (0.5 mm) thickness, to ensure the electrical insulation. The six heaters are all carefully mounted on a (350x350 mm^2) mica sheet and covered with other (350x350 mm^2) mica sheet to prevent the electrical contact, then covered together with a thin aluminium (0.3 mm) sheet. The heater placed on the copper plate.

3- Asbestos sheet of (6 mm) thick is fitted on the heater and covered with a glass wool of (50 mm) thickness and styrol-board to reduce the heat loss and then covered with an iron cover plate.

The power supply to the heating surface is an AC current 220 volts. A main automatic voltage regulator is connected to the circuit to insure that there is no fluctuation in the voltage within the test. The main power is controlled by six voltage regulators each one connected to one heating element fixed on the heating surface. These six voltage regulators are working to change the voltage supplied to the heating elements according to the temperature records in its location. This process is done as a feed back to the temperature reading in the region of the heater by the thermocouples which are builded in the copper plate in front of each heating element.

The cooling part as shown in **Fig. 3** consists of:-

1- An aluminium heat exchanger. This heat exchanger was formed from two separated parts. The first part which is mounted on the right side of the test section part is of (15 mm) thickness, with 15 channels each of (10mm) wide, feeding with water from the side by a water feeding pipe of (5 mm) in diameter and discharging the water from the other side by (5mm) in diameter pipe. The second part is of (5 mm) thickness aluminium sheet used to cover the first part. A rubber gasket is used to prevent water leaked from one channel to the other and to out.

2- The main constant temperature water supply source tube is connected to a header which is connected by 15 rubber tubes to the heat exchanger from each side inversely. The drain water comes out of the heat exchanger is discharging through 15 tubes connected to the down header, and then to the sink. A continuous water flow from the main supply is used and pumped through the heat exchanger, then drained without a return cycle. During the time period of this experimental work, the temperature degree of the main supply water was about 24^{o}C.

3- Six thermocouples, same kinds of the heating part, are fixed near the cooling surface of the heat exchanger from up to down in equally spaced. These thermocouples are used to monitor the temperature of the cooling part to maintain constant cooling temperature within ($\pm$1.1^{o}C), by adjusting the flow in each channel with the use of small gate valves maintained on each inlet water tube to the heat exchanger.

The test section part used in this study is a cubic box with 300x300x300mm^3 from inside. The four insulated walls are constructed from a 25 mm thickness mica sheet covered with a glass wool insulation of 50 mm thickness, and 50 mm thickness of styrol-board. The test section part is filled with silica sand and saturated with distilled water. The sand filtered between (0.4 to 0.6mm) diameter sizes.

The test section part temperature distribution was monitored with (68) thermocouples of the same kinds of that of the heating part. They are inserted and ceiled through 8 holes in the top side of the test section part, and located according to a designed plan as shown in **Fig. 4** to record the temperature change throughout the fluid saturated porous media. Two ports on the top side near the cooling part are used to feed saturated liquid, and another port on one side near the bottom used for feeding and drainage liquid. The entire test rig was fixed on a variable angle of inclination frame, to allow inclining the box with the desired angle.

The effective thermal conductivity of the solid-fluid combination which forms the saturated porous media, can be evaluated by,

$$k_{eff.} = k_s^{1-\varepsilon} . k_f^{\varepsilon} \quad (1)$$

This provides a good estimate as long as k_s and k_f are not too different from each other **(Nield 1991).**

The heat capacity of the fluid-solid combination of the saturated porous media can be evaluated as the weighted arithmetic mean of fluid and solid heat capacity, according to,

$$(\rho C)_m = \varepsilon(\rho c_p)_f + (1-\varepsilon)(\rho C)_s \quad (2)$$

$(\rho C)_m$ = mean heat capacity of the media.

$(\rho c_p)_f$ = fluid saturated heat capacity.

$(\rho C)_s$ = solid matrix heat capacity.

The specific heat of the silica sand is obtained from Poirier thermal tables for matters. It is equal to ($C = 1170\, J/kg^oK$). The constant pressure specific heat of the distilled water is obtained from (Holman 1985) according to the mean temperature of the cold and hot surfaces for each constant temperature test run.

Modified Rayleigh number *(Ra)* is used as a main parameter upon which the thermal distribution within the saturated porous media depends. For constant temperature boundary conditions,

$$Ra = \frac{g\beta K(\rho C)_m \Delta T_o L_x}{\nu_f k_{eff.}} \quad (3)$$

There are many reasons limited the Rayleigh number values in this work:

1- The porous media was the silica sand which has a very low permeability.

2- The boiling point of the saturated fluid (distilled water) is (100°C).

3- This work was designed for a single phase flow.

4- The boundary condition specified as constant heating temperatures, which must not exceed (100°C).

For all these reasons, the modified Rayleigh number for the experimental work does not exceed more than (*Ra*=55) which is the number obtained when maximum constant temperature (T_h=100°) is allowed on the heating side and minimum allowed water source temperature of (24°C).

Nusselt number assumed to be reference to the effect of fluid motion on heat transfer. It is of a great interest to study this effect by determining Nusselt number in each stage of heat transfer process within a cavity of saturated porous media.

$$Nu = \frac{h.L_z}{k_{eff.}} = \frac{-\left.\frac{\partial T}{\partial Z}\right|_{z=0} L_z}{\Delta T_o} \quad (4)$$

In this work, the hot surface is divided into (25) elements, by dividing the X-length and the Y-length into five parts. For each one of these (25) elements, $\left.\frac{\partial T}{\partial Z}\right|_{z=0}$ assumed to be constant and calculated according to the experimental data of (temperature distribution), using the one-sided difference formula. ΔT_o is calculated for each element as the difference between the measured temperature at the centre of this element and the cooling surface constant temperature which is equal to (24°C). At last, the average Nusselt number is calculated as the average of (25) elementals Nusselt numbers.

$$Nu_{average} = \frac{1}{A}\int Nu.dA \quad (5)$$

RESULTS AND DISCUSSION

The experimental work is limited to Rayleigh numbers of (Ra = 55, 42, 32, 21, and 14) related to the constant heating surface temperature of (T_h = 100, 90, 80, 70, and 60°C) and constant cooling surface temperature of (24°C). These five Rayleigh numbers are examined in four inclination angles of (θ = 0, 15, 30 and 45°) so that a total of 20 experimental runs have been done. All experimental results are plotted in contour maps using dimensionless temperature referring to the cold side temperature, and dimensionless distance referring to the side length of the cubic box. Each experimental run gets (7 to 8 hours) to reach steady state condition. The recording of the temperature distribution is stared 10 minutes from the beginning of the experimental run, and then each half an hour. The definition of steady state condition is fixed as the temperature difference of the last two readings, of any probe in the enclosure must not exceed (0.2°C). To simplify showing the countor maps of the transient temperature distribution throughout the section, selected time intervals (recording

temperatures) have been made from the total experimental recording temperatures, according to the time rate of change of the temperature distribution. Therefore, the dimensionless of the time intervals of the experimental works are specified as (t=0.04, t=0.1, t=0.16, and t=steady state time).

Section (1) in **Fig. 4** which is located (30mm) distance from the heating side in the *Z*-direction, used to measure the temperature gradient at the heating surface so that Nusselt number can be deduced experimentally and assists in plotting the temperature distribution map in the other sections. Section (2) which is located (60mm) from the cold side in the *Z*-direction used only to monitor the behaviour of the temperature distribution near the cold surface and assists in plotting the temperature distribution map in the other sections. Section (3) is located (150mm) in the *Y*-direction which connects the heating and cooling sides, and represents the most useful section showing the behaviour of the isothermal lines through the porous media. Section (4) is located (150mm) in the *X*-direction and section (5) is located (150mm) in the *Z*-direction. These two sections are used to show the symmetry of the temperature distribution throughout the enclosure in these plans.

The contour maps of **Fig. 5** represent the transient temperature distribution on section (3). The constant heating side temperature maintained at (100^{o}C) equivalents to ($Ra = 55$). The contour-maps describe the change of dimensionless temperature with dimensionless heat flow direction distance (*Z*-direction). In this figure, the time change of the temperature distribution at an inclination angle ($\theta = 0^o$), is represented by (A,B,C,D). At the starting time of the experiment, a huge amount of heat is transferred near the heating surface by conduction, and some is gone deeper in the saturated porous media by convection and conduction due to the low heat resistance, and sudden attack of the heat, causes irregular isothermal lines as shown in the figure (map-A). This irregularity is soon transferred to regular isothermal lines at the second time step (map-B). At this step, a progression in the isothermal lines is shown towards the cooling surface in a curvilinear form refers to the circulation of the saturated fluid in the clockwise direction in the enclosure, which means that heat is transferred by convection. It is shown in (map-C) that more heat is transferred and the temperatures of all isothermal lines are increased. When the situation of the saturated porous media is coming soon to be steady state, the rate of temperature rising of the isothermal lines is reduced as shown in (map-D). The curvature of the isothermal lines at the bottom and at the top of the enclosure refers to the convection heat transfer who occurs at these ends, whereas the semi-constant slop parts of these isothermal lines at the middle region refers that the fluid is stagnant. The figure also shows the influence of the angle of inclination of the enclosure on the temperature distribution pattern. The curvature of the isothermal lines is increasing as the inclination angle increases referring to the increases in the natural convection heat transfer rate. It is clear that the rate of change of the curvature of the isothermal lines reduces steeply as (θ) approaches ($\theta = 45^o$), which means that this is an inversion inclination angle. The influence of inclination angles is represented by the effect of the gravity acceleration component which is aligned with the flow in all directions produced a vigorous fluid circulation. This can be illustrated by comparing the steady state maps of figure (5:D,H,L,P).

Figs. 6 and **7** show the effects of decreasing the temperature of the heating side to (T_h= 80, and 60^{o}C) or decreasing Rayleigh number to ($Ra = 32$, and 14), respectively. It is clear that the convection heat transfer is reduced steeply as Rayleigh number reduced. This can be noted from these figures according to the shape of the isothermal lines which tend to be straight lines instead of curvilinear as Rayleigh number decreases. **Fig. 7** for Ra=14 shows that most heat transfer is occurred by conduction, as the isothermal lines are nearly straight lines.

To deduce experimentally the effect of Rayleigh number and inclination angles on the behaviour of time change of average Nusselt number, each an hour time interval of the experimental runs, average Nusselt number has been measured.

Figs. 8 to 10 show the relation between average Nusselt number with dimensionless time for ($Ra = 55$, 32, and 14), respectively at different inclination angles ($\theta = 0$, 15, 30, and 45^o), and figures (11) to (13) shows this relation for different inclination angles ($\theta = 0$, 30 and 45^o), respectively

at different ($Ra = 55$, 42, 32, 21, and 14). All these figures show that average Nusselt number is rapidly decreased with time, at a short time period from the beginning of the test run, and then average Nusselt number continuously reduced with time but with a less step, forming a parabolic shape. This behaviour is related to the reduction in the amount of heat transfer from the heating side to the saturated porous media due to the increase in the thermal resistance as the temperature of the saturated porous media increases with time. **Fig. 8** shows the relation for (T_h=100°C) or ($Ra = 55$). It is shown that, as inclination angle of the enclosure is increased, the time change of average Nusselt number shifts to up, recording that there is a vigorous convective flow that diffuse the heat more effectively within the cavity. But at ($\theta = 45^o$), the time change of average Nusselt number comes done slightly indicating an inversion point. **Figs. 9** and **10** for ($Ra = 32$, and 14), respectively indicating close lines of average Nusselt number time change, especially when the state comes to be steady due to the semi-absent of the convection phenomenon. **Figs. 11 to 13** show that increasing Rayleigh number due to the increase in the temperature of the heating side, causes an increase in the average Nusselt number due to the increase in the amount of heat that can be transferred to the saturated porous media from this side. This is true for all inclination angles. **Fig. 14** shows the relation between average Nusselt number with the dimensionless time, Rayleigh number, and inclination angle. In order to transfer this graphic relation to correlation equation, the average Nusselt number can be written as follows,

$$Nu = C[t^{-m}(Ra\cos\theta)^n] \qquad (6)$$

Statistical analysis using (Statistica Software Version 6.0) was used to specify the constants (*C*, *m*, and *n*). The result is,

$$Nu = 0.231737[t^{-0.455}(Ra\cos\theta)^{0.3}] \quad (7)$$

The correlation coefficient is (R=0.96757). This value is valid in the range of (*Ra*=14 to 55) and inclination angle ($\theta = 0$ to 45°).

Figs. 15 and **16** show the relation between local Nusselt numbers verses dimensionless X-distance at steady state time for ($Ra = 55$, and 21), respectively with different inclination angles ($\theta = 0$, 15, 30, 45°). From these figures, it is clear that increasing the inclination angle increases local Nusselt number in all locations. This effect is reduced as Rayleigh number reduced due to the reduction in the influence of convection heat transfer. This situation can be noticed by the convergence between the relation curves for different inclination angles, the curves being more straights as Rayleigh number reduced. It is also clear from these figures that inclination angle ($\theta = 45^o$) is an inversion angle at which Nusselt number reduced at all locations. **Fig. 17** shows the relation between local Nusselt number with dimensionless X-distance, and ($Ra\cos\theta$). This relation is transformed to correlation equations and gives the following forms:

$$Nu = 0.475937[X^{-0.27} + (Ra\cos\theta)^{0.13}] \qquad (8)$$

This correlation is for Rayleigh number ($Ra = 32$ to 55) and inclination angle ($\theta = 0$ to 45°), with (R=0.8903), and,

$$Nu = 0.453262[X^{-0.225} + (Ra\cos\theta)^{0.08}] \quad (9)$$

is for Rayleigh number ($Ra = 14$ to 21) and inclination angle ($\theta = 0$ to 45°), with (R=0.9031).

Fig. 18 shows the average Nusselt number verses ($Ra\cos\theta$) at steady state time for all 20 tests. The curve fitting for this relation gives a general correlation equation as follows:-

$$Nu = 0.4727 + 0.6277 * \log_{10}[Ra\cos(\theta)] \quad (10)$$

This correlation is valid for ($14 \le Ra \le 55$) and ($0^o \le \theta \le 45^o$) with (R=0.9083).

CONCLUSIONS

Rayleigh numbers range applied in this work is limited to (*Ra*=14 to 55) according to the constant heating temperature limits of (T_h=60 to 100°C) and the low permeability of the silica sand. Angles of inclination of the enclosure applied are ($\theta = 0^o$, 15°, 30°, and 45°). The main conclusions are: Heat transfer regime is mainly conduction for all Rayleigh numbers with a small influence of convection for ($Ra = 42$) and a greater for ($Ra = 55$). This effect increases with the angle of

inclination of the enclosure. For all Rayleigh numbers, the core of the enclosure is in the conduction heat transfer regime. Average Nusselt number decreases with time until reached steady state condition. Average Nusselt number increases with Rayleigh number and/or inclination angle of the enclosure. Silica sand as porous media limited the wideness of the Rayleigh numbers under investigation and reduced the convection flow heat transfer. Increasing the inclination angle increases local Nusselt number in all locations on the hot surface. This effect is reduced as Rayleigh number reduced.

REFERENCES

- Beg, O. A., Takhar, H. S., Soundalgekar, V. M., and Prasad, V., "Thermo-convective Flow in a Saturated, Isotropic, Homogeneous Porous Medium Using Brinkman's Method: Numerical Study", Int. J. of Numerical Methods for Heat and Fluid Flow, Vol.8, No.5, PP.559-589, (1998).

- Holman, J. P., "Heat Transfer", Fifth Edition, McGraw-Hill International Book Company, (1985).

- Horton, C. W., and Rogers, F. T., Journal Applied Physics, 16, 360, (1945).

- Lapwood, E. R., and Proc. Camb. Phil. Soc. 44, 508, (1948).

- Nield, D. A., "Estimation of the Stagnant Thermal Conductivity of Saturated Porous Media", Int. J. Heat Mass Transfer, 34, PP.1575-1576, (1991).

- Nield, D. A., and Bejan, A., " Convection in Porous Medium", Third edition 2006 springer Science Business Media, Inc.

- Prasad, V., Kulacki, F. A., and Keyhani, M., "Natural Convection in Porous Media", J. Fluid Mech. Vol.150, PP.89-119, (1985).

- Vafai, K., "Hand Book of Porous Media", Second Edition Published by Taylor and Francis Group, (2005).

NOMENCLATURES

A	Cross sectional area , m^2
C	Specific heat, kJ/kg.^{o}C
C_p	Specific heat at constant pressure, kJ/kg.^{o}C
g	Gravitational acceleration, m/s^2
L_x	Side length of the box in x-direction, m
k	Thermal conductivity, W/m.^{o}C
K	Permeability, m^2
Nu	Nusselt number
$Nu_{av.}$	Average Nusselt number
Ra	Modified Rayleigh Number
t	Dimensionless time
T	Dimensional value of the temperature, ^{o}C
T_o	Reference temperature, ^{o}C
ΔT_o	Temperature difference ($T_h - T_c$), ^{o}C
α_m	Thermal diffusivity of the porous medium, m^2/s
β	Thermal volume expansion coefficient, 1/K
ε	Porosity (fraction of the total media volume occupied by fluid)
$1-\varepsilon$	(fraction of the total media volume occupied by solid matrix)
ν	Kinematics viscosity, m^2/s
θ	Inclination angle, degree
ρ	Density, kg/m^3
eff.	Effective
f	Fluid
m	Medium
s	Solid
ref	Reference

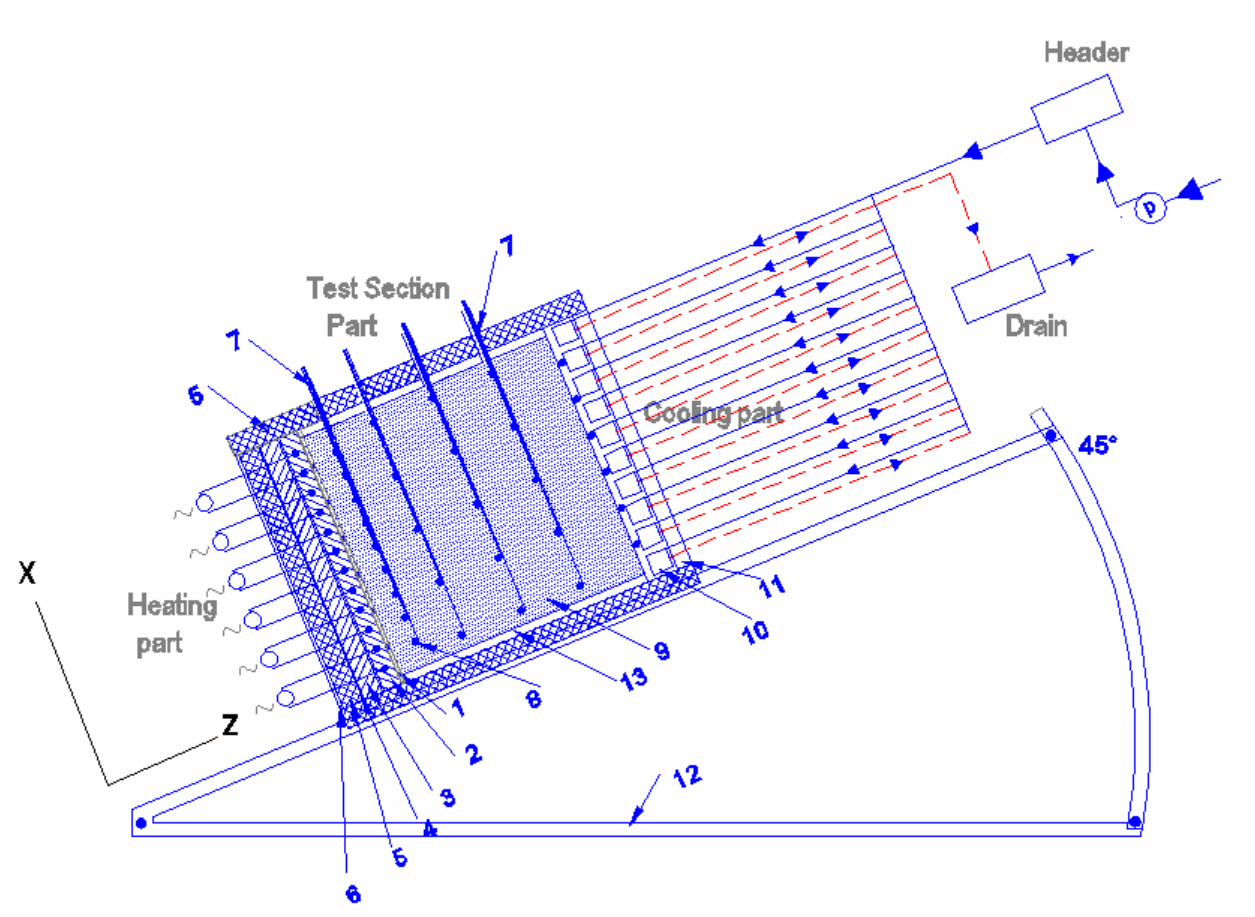

1	5mm copper plate
2	Main Heater (6 parts)
3	Asbestos 5mm thick
4	Aluminium plate 3mm thick
5	Insulation material
6	Cover plate 3mm thick
7	Thermocouple ports
8	Thermocouple
9	Saturated silica sand
10	Aluminum groves plate
11	Aluminum cover plate 5mm thick
12	Variable angle Frame
13	Mica box 25 mm thickness

Fig.1: Schematic Diagram of the Experimental Test Rig

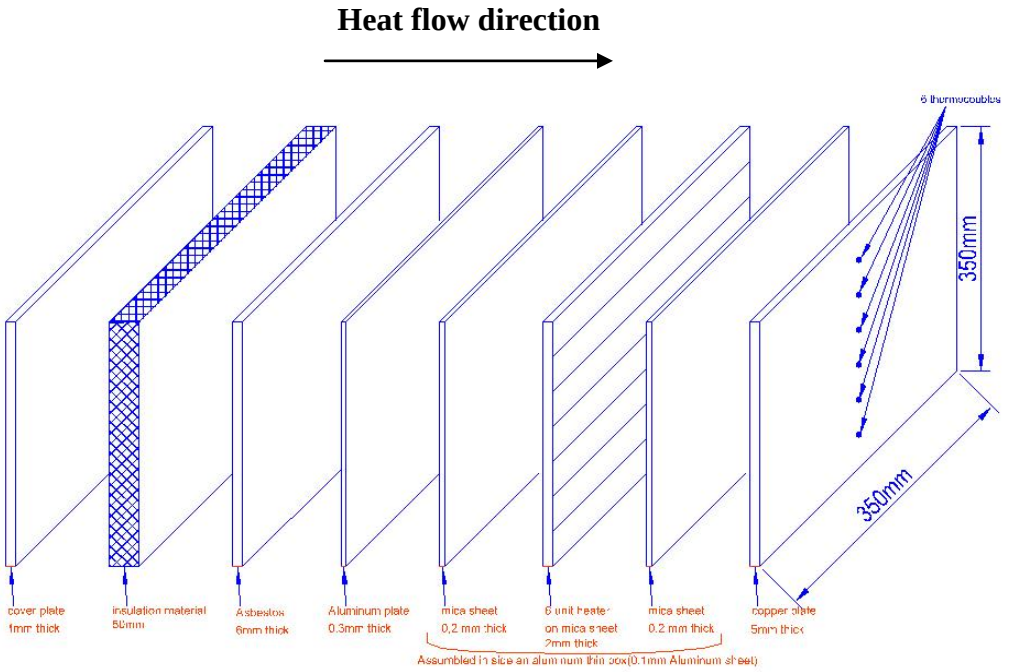

Ingredients of the Heating Part

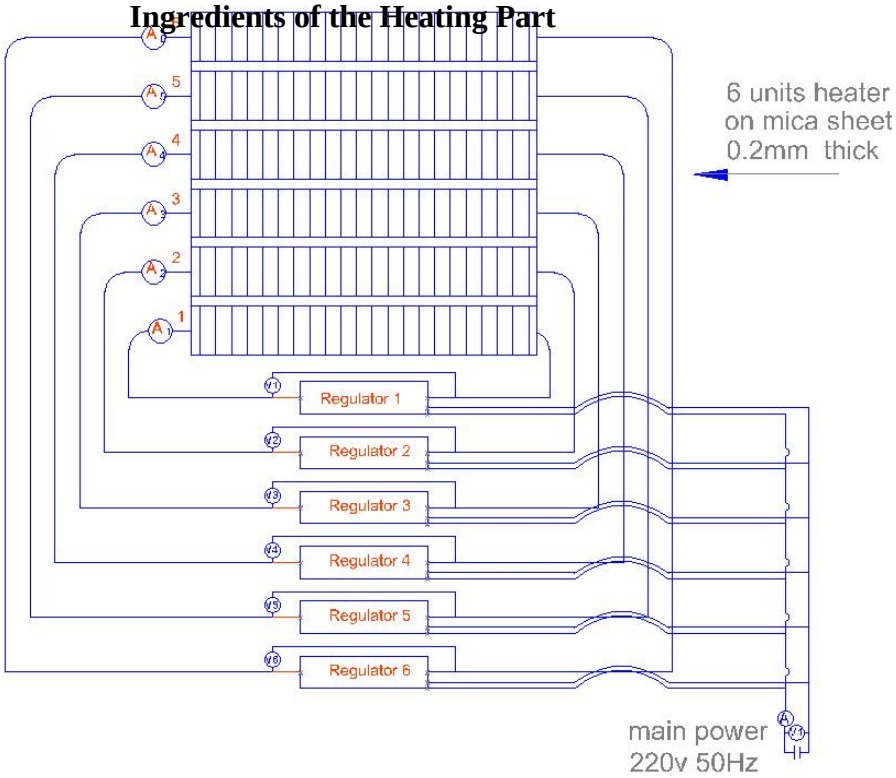

Schematic Diagram for the Electrical Heaters Connection

Fig.2: Heating Part

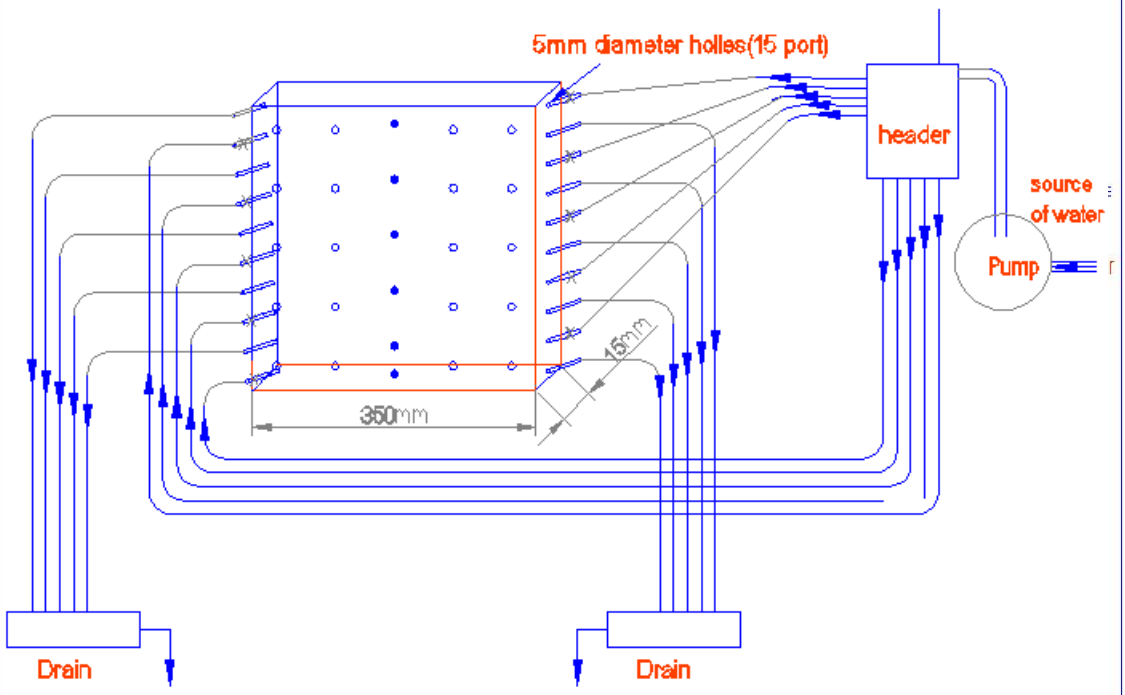

Schematic Diagram of the Cooling Part

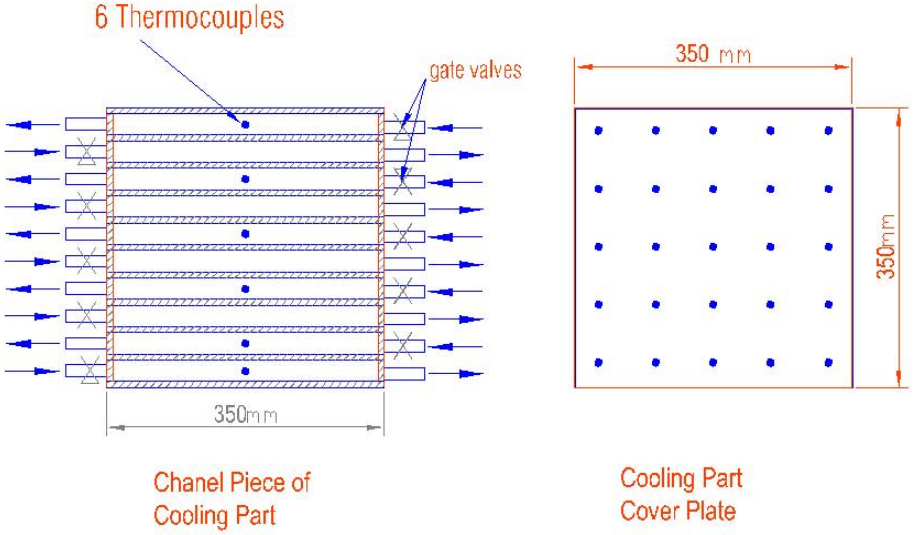

Fig.3: Cooling Part

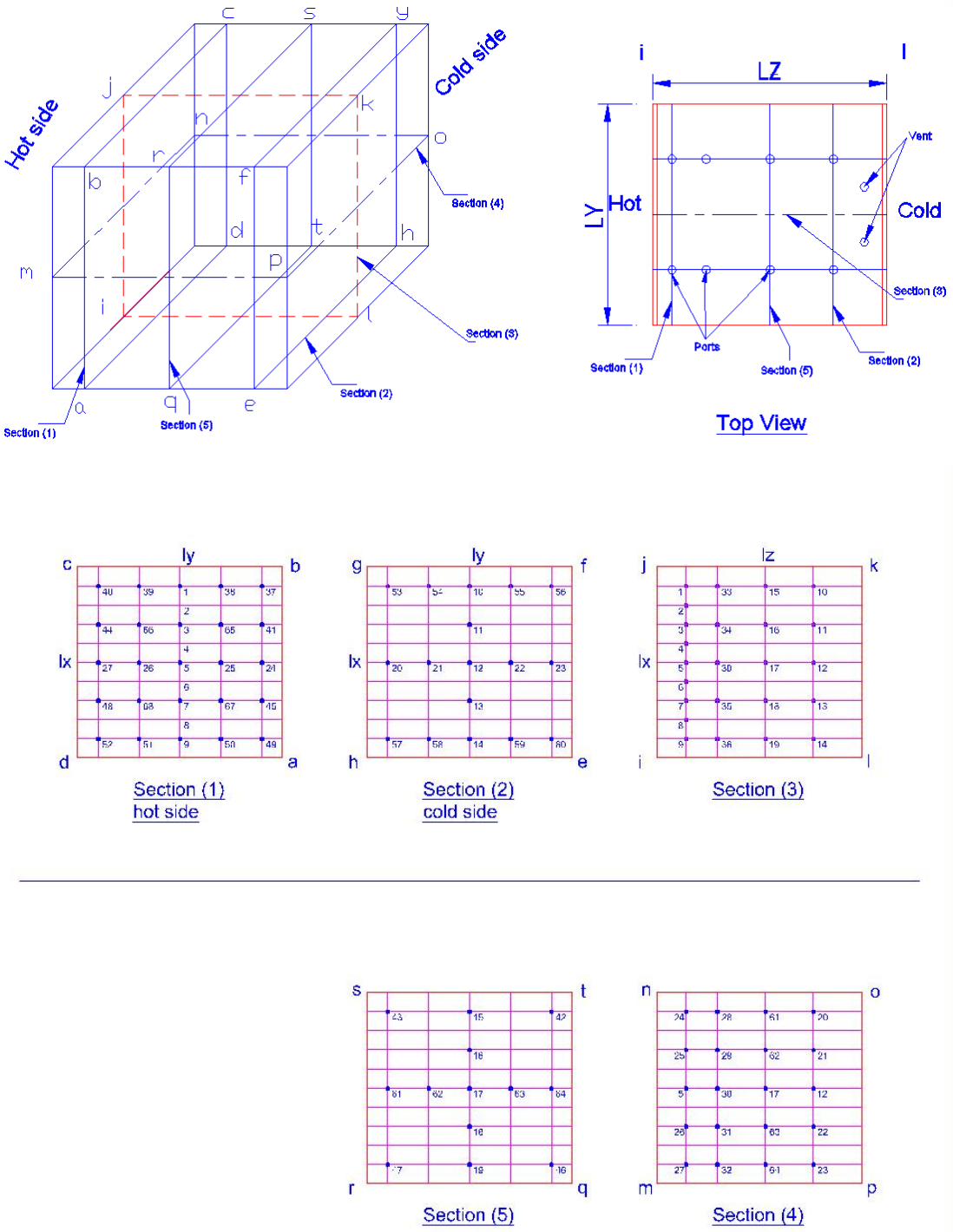

Fig.4: Test Section Part and Thermocouples Distribution

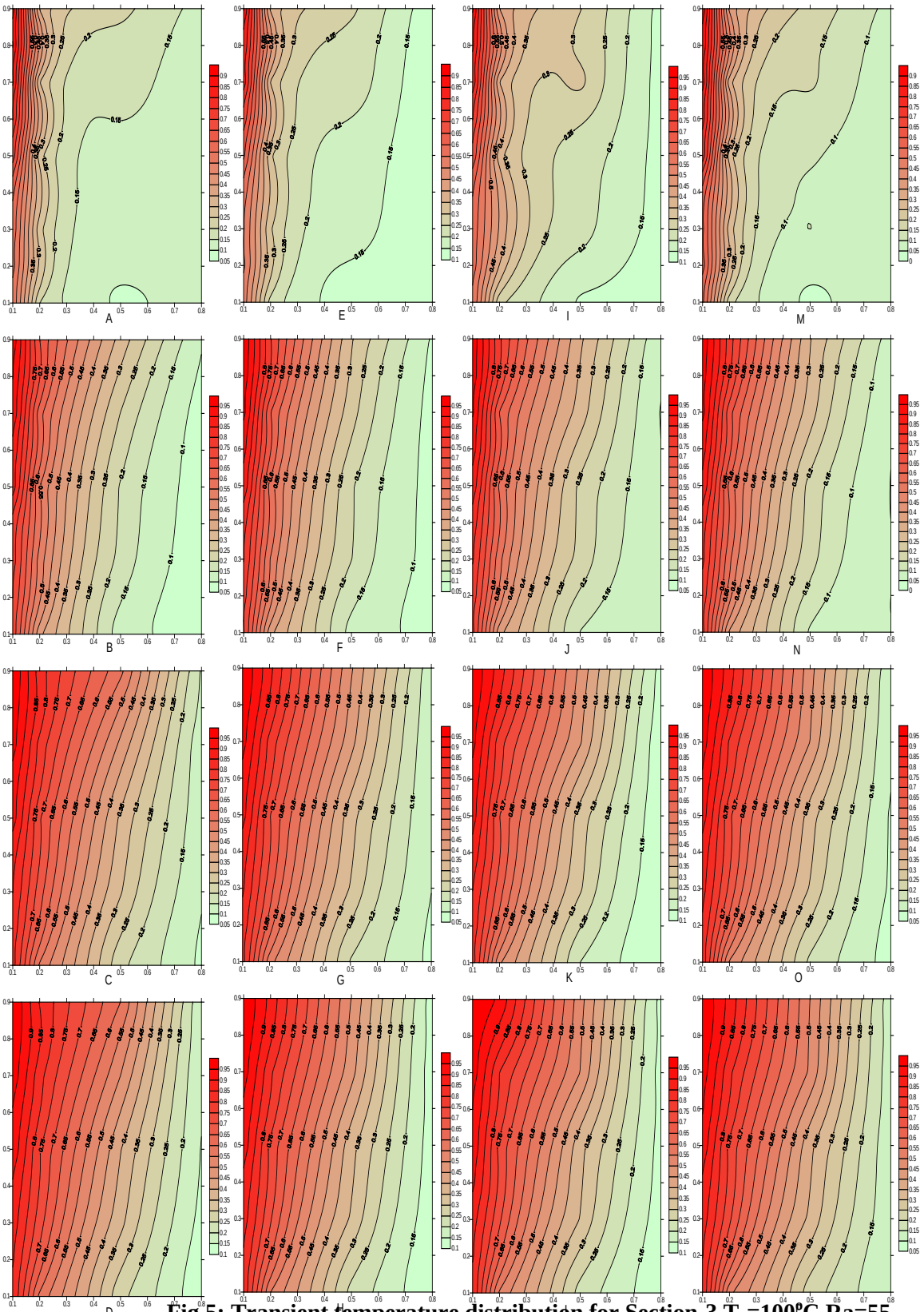

Fig.5: Transient temperature distribution for <u>Section-3</u> T_h=100°C Ra=55, θ=0° :(A,B,C,D), θ=15° :(E,F,G,H), θ=30° :(I,J,K,L), θ=45° :(M,N,O,P) t=0.04:(A,E,I,M), t=0.1 :(B,F,J,N), t=0.16 :(C,G,K,O), t=steady state :(D,H,L,P)

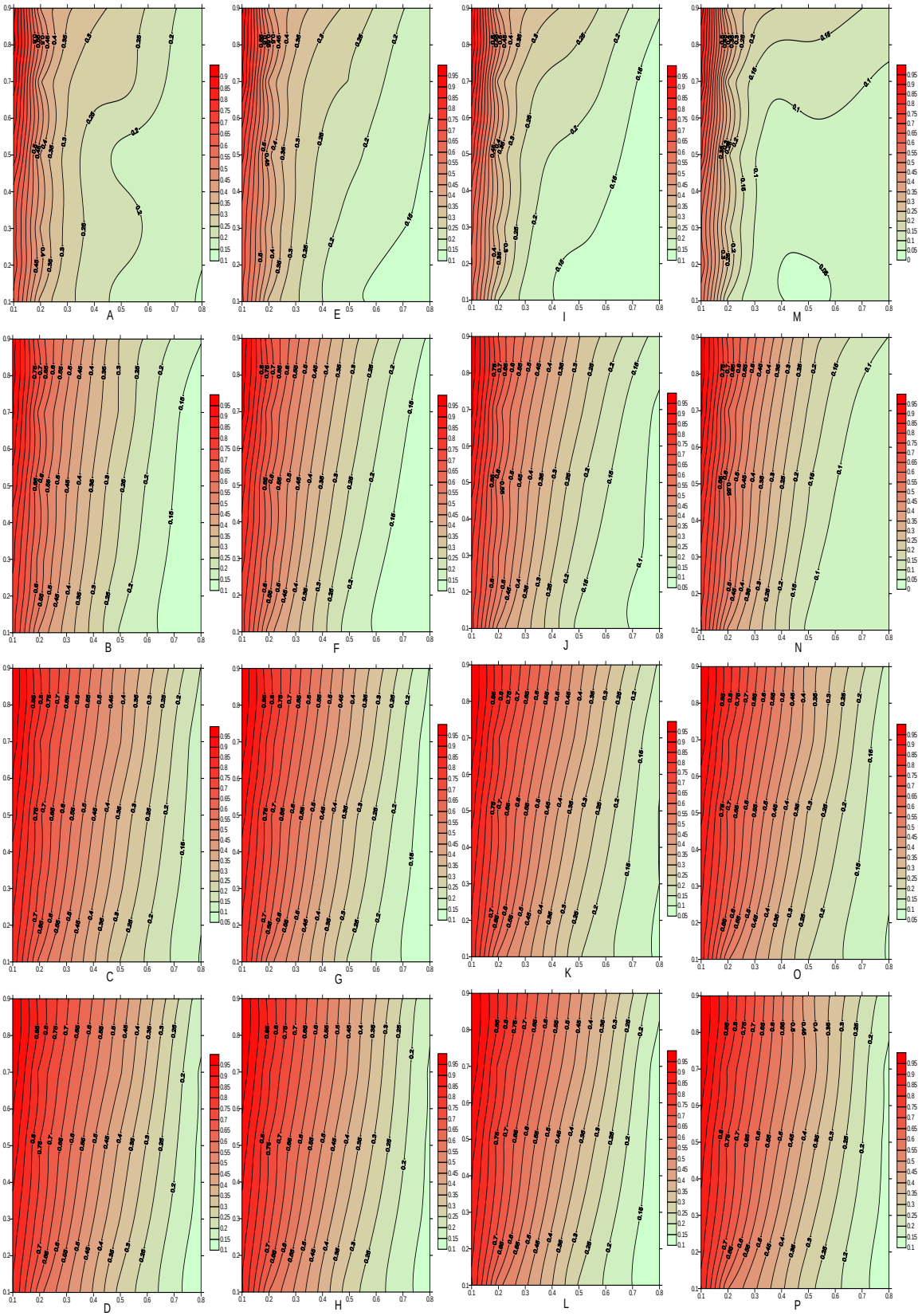

Fig.6: Transient temperature distribution for <u>Section-3</u> T_h=80°C Ra=32, θ=0° :(A,B,C,D), θ=15° :(E,F,G,H), θ=30° :(I,J,K,L), θ=45° :(M,N,O,P) t=0.04:(A,E,I,M), t=0.1 :(B,F,J,N), t=0.16 :(C,G,K,O), t=steady state :(D,H,L,P)

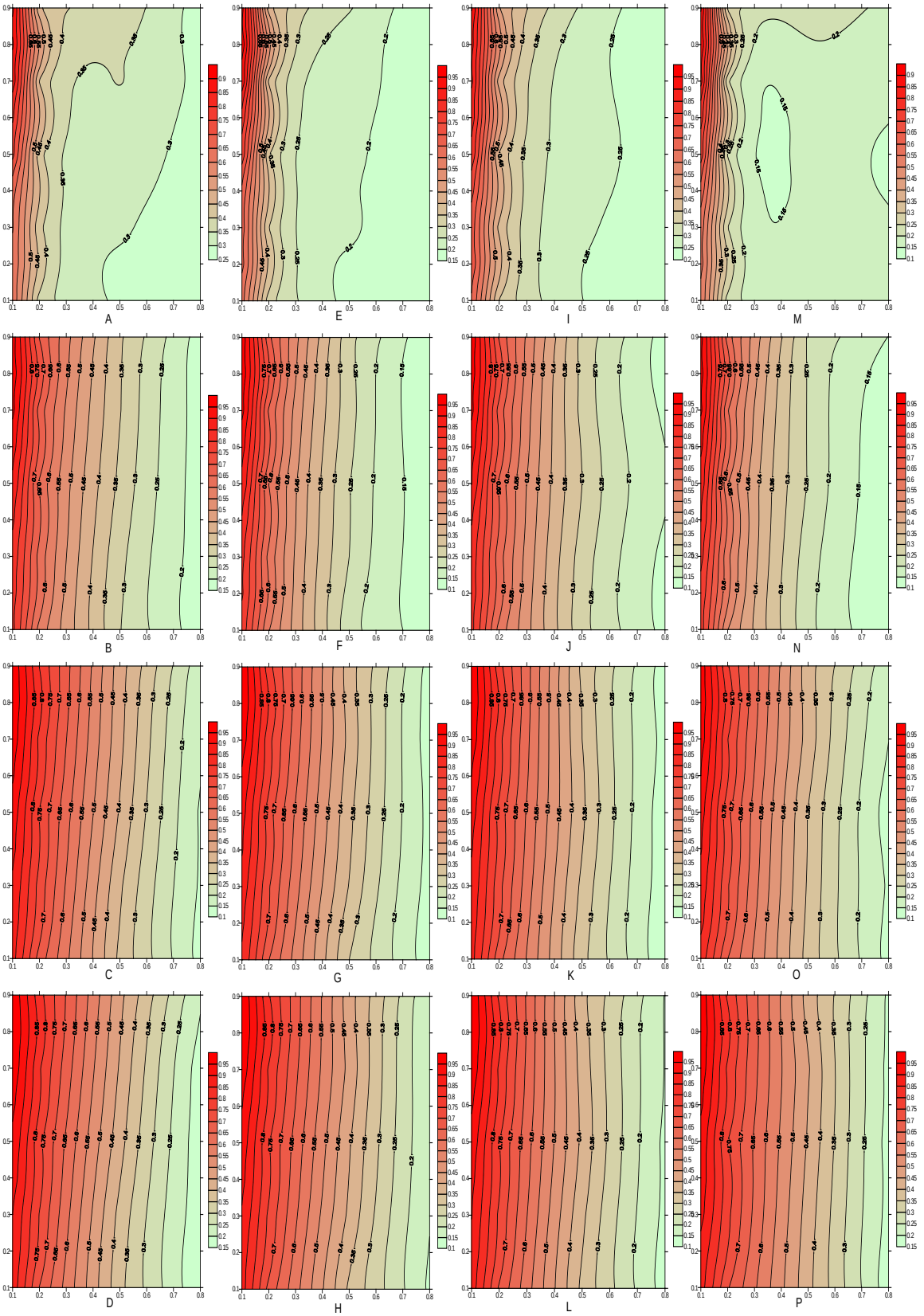

Fig.7: Transient temperature distribution for <u>Section-3</u> T_h=60°C Ra=14, θ=0° :(A,B,C,D), θ=15° :(E,F,G,H), θ=30° :(I,J,K,L), θ=45° :(M,N,O,P) t=0.04:(A,E,I,M), t=0.1 :(B,F,J,N), t=0.16 :(C,G,K,O), t=steady state :(D,H,L,P)

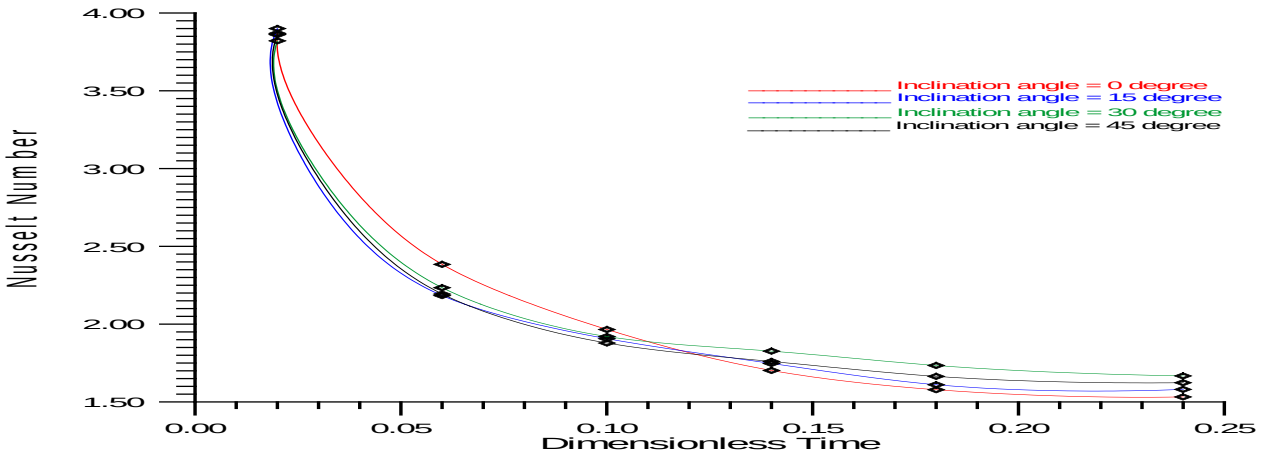

Fig.8: Average Nusselt number verses Dimensionless time for Ra=55 or T_h=100^{o}C, for various values of inclination angles.

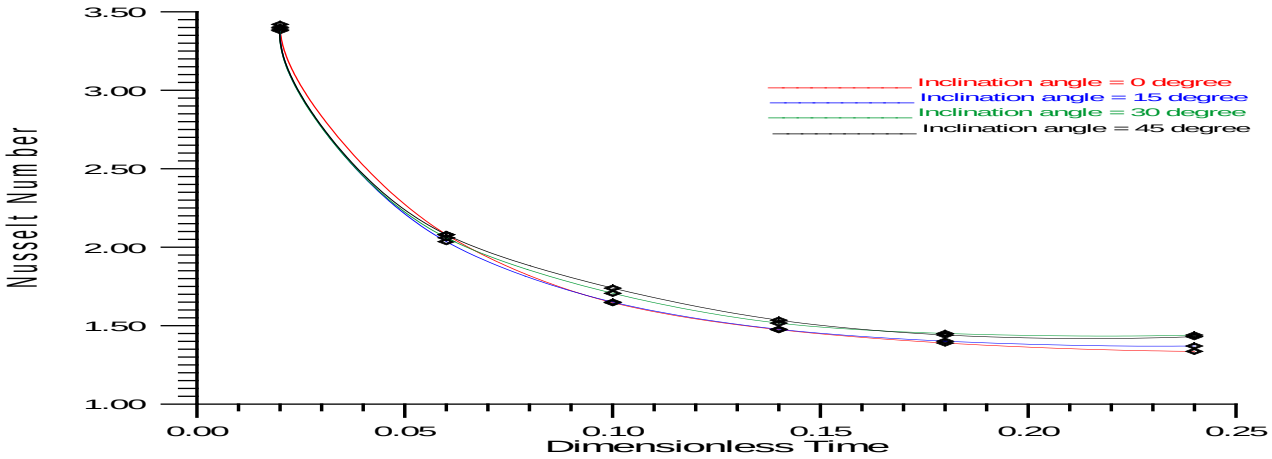

Fig.9: Average Nusselt number verses Dimensionless time for Ra=32 or T_h=80^{o}C for various values of inclination angles

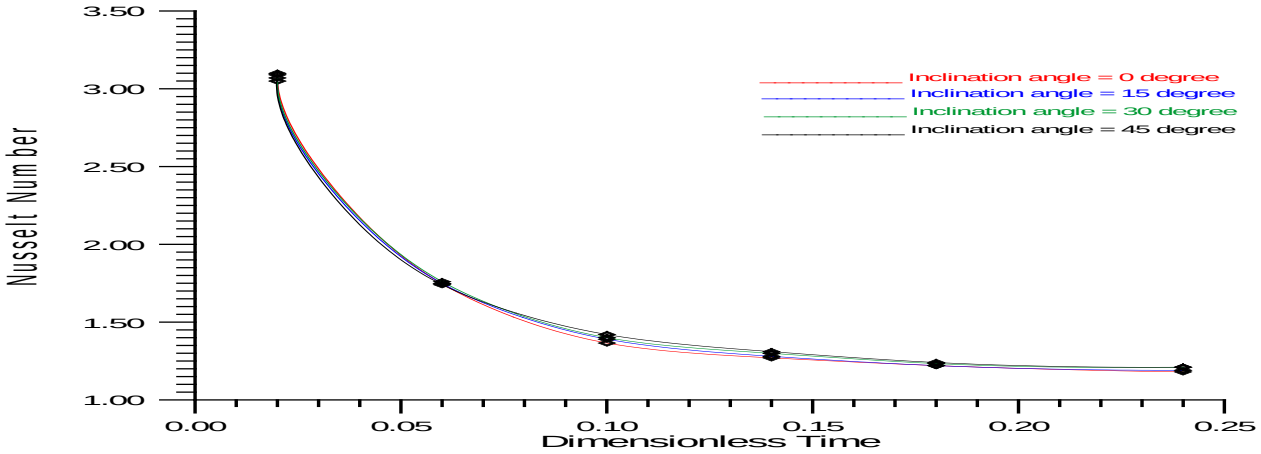

Fig.10: Average Nusselt number verses Dimensionless time for Ra=14 or T_h=60^{o}C for various values of inclination angles

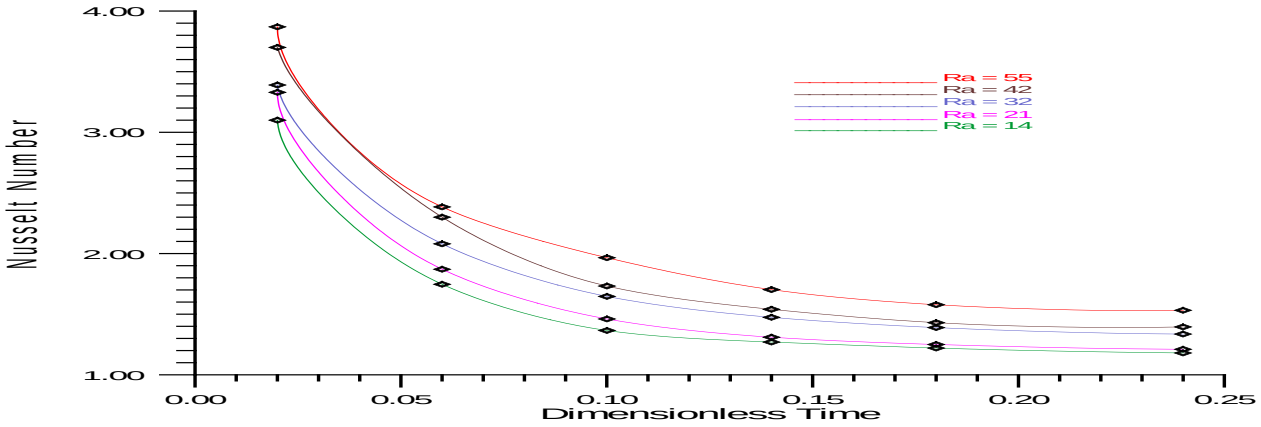

Fig.11: Average Nusselt number verses dimensionless time at an inclination angle θ=0° for various values of modified Rayleih number or hot surface constant temperature (Ra=55 or T_h=100°C, Ra=42 or T_h =90°C, Ra=32 or T_h =80°C, Ra=21 or T_h =70°C, Ra=14 or T_h =60°C)

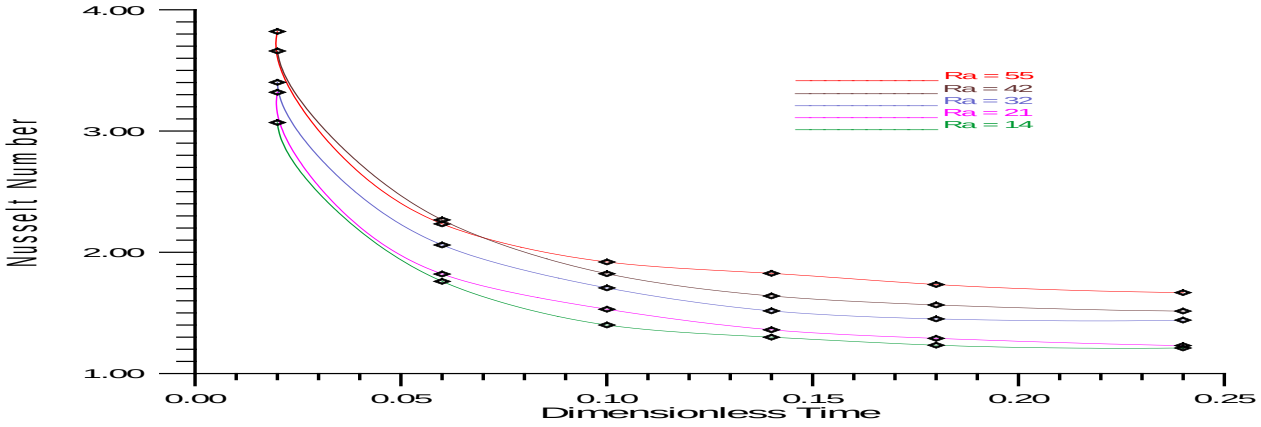

Fig.12: Average Nusselt number verses dimensionless time at an inclination angle θ=30° for various values of modified Rayleih number or hot surface constant temperature (Ra=55 or T_h=100°C, Ra=42 or T_h =90°C, Ra=32 or T_h =80°C, Ra=21 or T_h =70°C, Ra=14 or T_h =60°C)

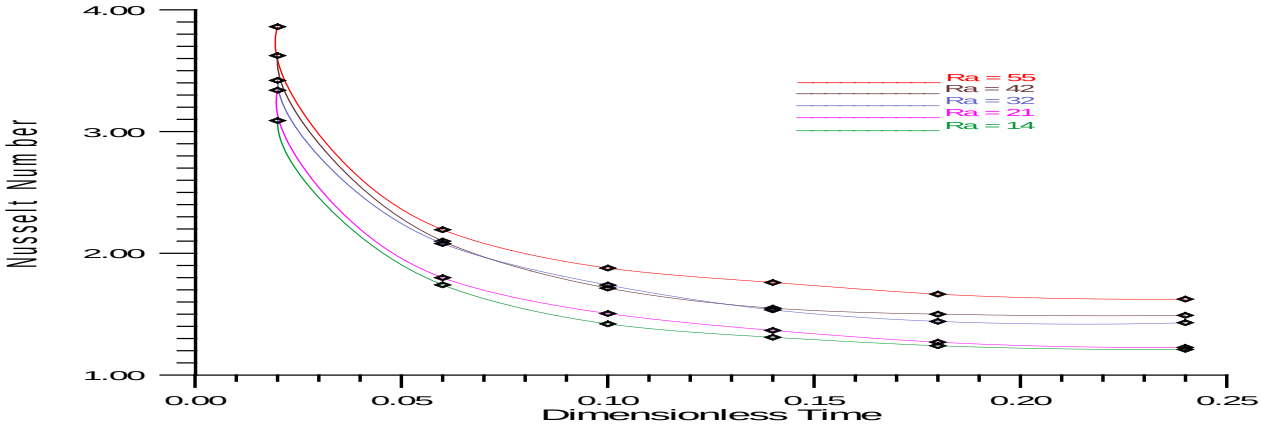

Fig.13: Average Nusselt number verses dimensionless time at an inclination angle θ=45° for various values of modified Rayleih number or hot surface constant temperature (Ra=55 or T_h=100°C, Ra=42 or T_h =90°C, Ra=32 or T_h =80°C, Ra=21 or T_h =70°C, Ra=14 or T_h =60°C)

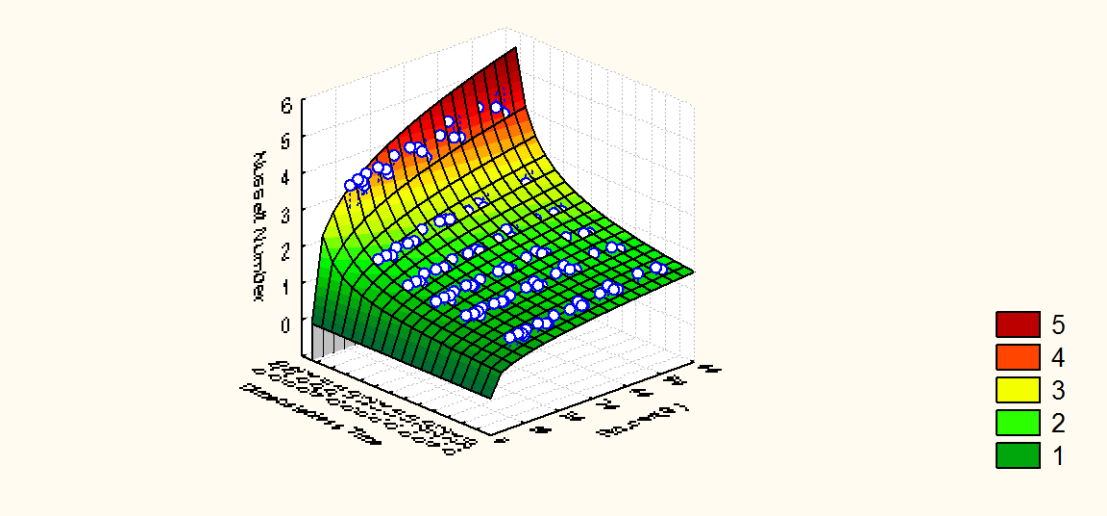

Fig.14: Average Nusselt number verses dimensionless time at an inclination angle θ =0 to 45° for modified Rayleigh number or hot surface constant temperature Range (Ra=14 to 55 or T_h=60 to100°C)

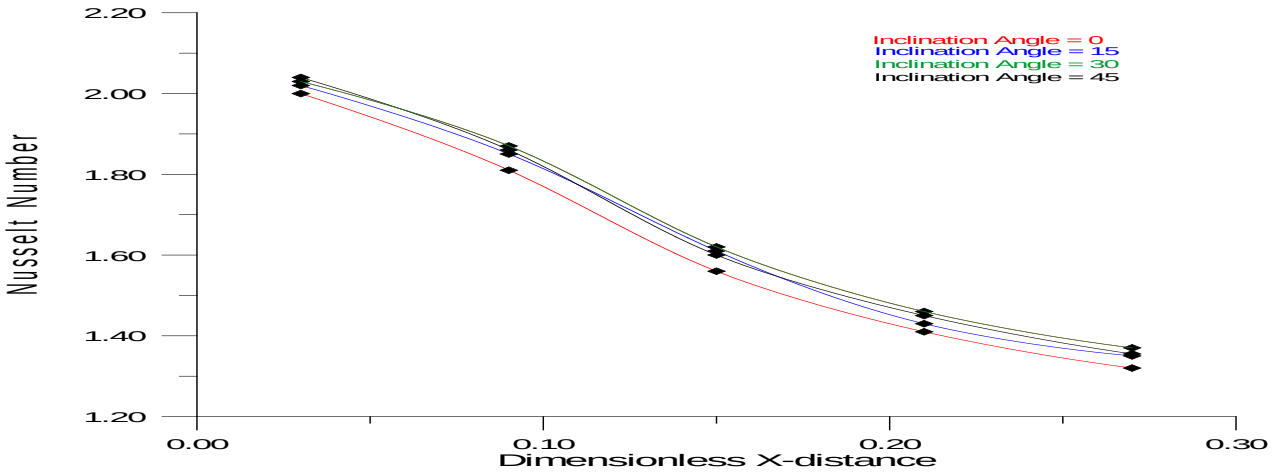

Fig.15: Local Nusselt Number verses dimensionless X-distance at steady state time for Ra=55 or T_h=100°C for various values of inclination angles

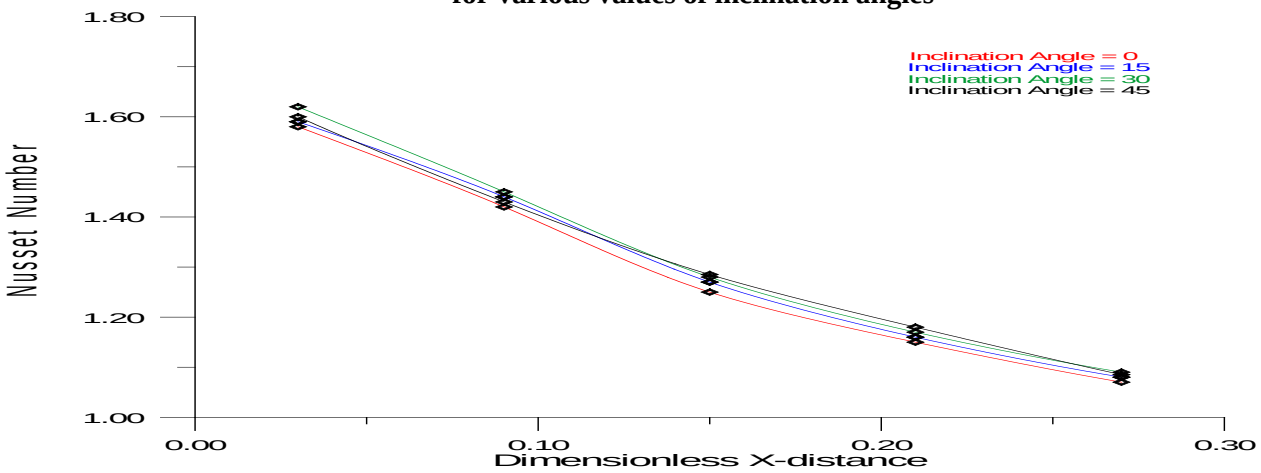

Fig.16: Local Nusselt Number verses dimensionless X-distance at steady state time for Ra=21 or T_h=70°C for various values of inclination angles

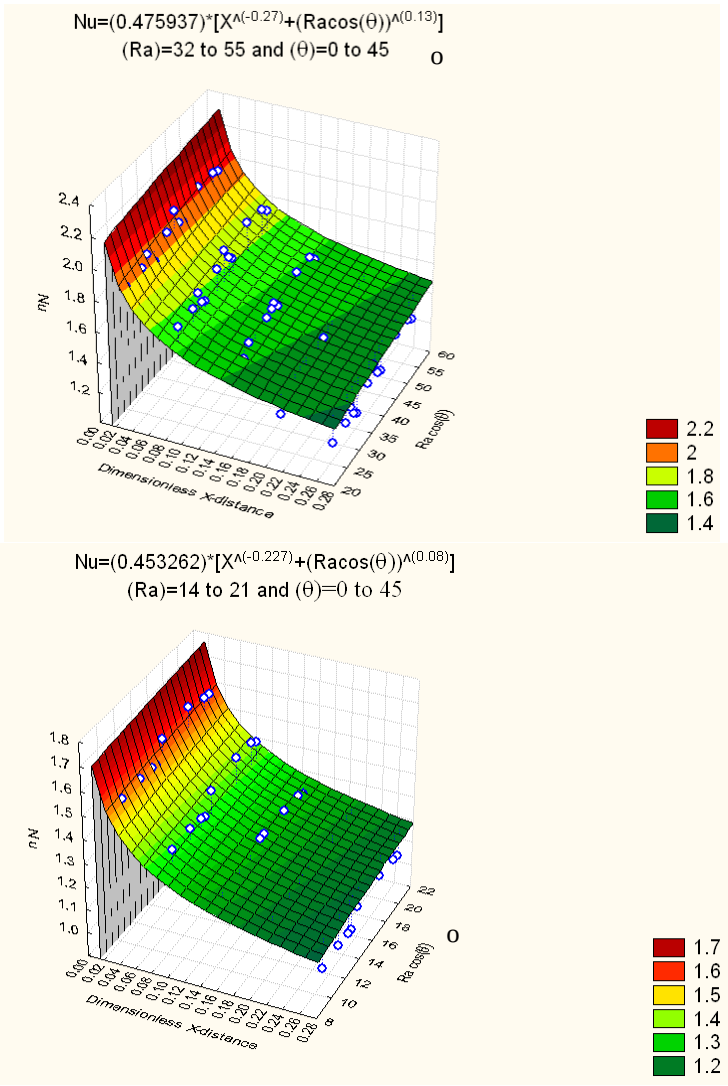

Fig.17: Local Nusselt Number verses dimensionless X-distance at steady state time for Ra=32 to 55 and for Ra= 21 to 14 and θ=0 to 45°

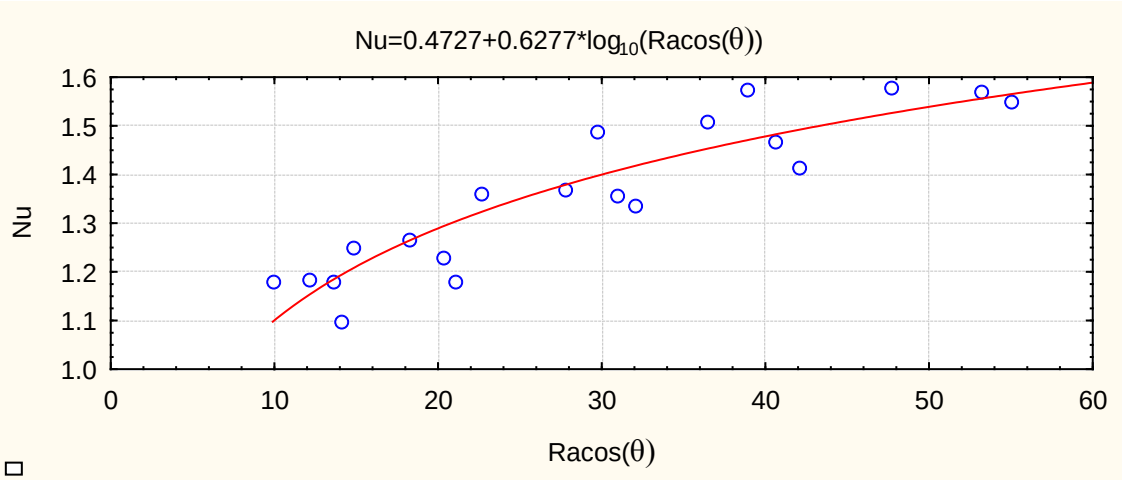

Fig.18: Steady state Average Nusselt Number verses [$Ra\cos(\theta)$] at $(0 \le \theta \le 45^{\circ})$ for (14<Ra<55), R=0.9083